Published in final edited form as:
J Biol Chem. 2008 January 4; 283(1): 145–154. doi:10.1074/jbc.M704060200.

hMSH4-hMSH5 Adenosine Nucleotide Processing and Interactions with Homologous Recombination Machinery*

Timothy Snowden[‡], **Kang-Sup Shim**[§], **Christoph Schmutte**[§], **Samir Acharya**[§], and **Richard Fishel**[§,1]

[‡]Genetics and Molecular Biology Program, Kimmel Cancer Center, Philadelphia, Pennsylvania 19107

[§]Molecular Virology, Immunology, and Medical Genetics, Human Cancer Genetics, The Ohio State University School of Medicine and Public Health, Columbus, Ohio 43210

Abstract

We have previously demonstrated that the human heterodimeric meiosis-specific MutS homologs, hMSH4-hMSH5, bind uniquely to a Holliday Junction and its developmental progenitor (Snowden, T., Acharya, S., Butz, C., Berardini, M., and Fishel, R. (2004) *Mol. Cell* 15, 437–451). ATP binding by hMSH4-hMSH5 resulted in the formation of a sliding clamp that dissociated from the Holliday Junction crossover region embracing two duplex DNA arms. The loading of multiple hMSH4-hMSH5 sliding clamps was anticipated to stabilize the interaction between parental chromosomes during meiosis double-stranded break repair. Here we have identified the interaction region between the individual subunits of hMSH4-hMSH5 that are likely involved in clamp formation and show that each subunit of the heterodimer binds ATP. We have determined that ADP → ATP exchange is uniquely provoked by Holliday Junction recognition. Moreover, the hydrolysis of ATP by hMSH4-hMSH5 appears to occur after the complex transits the open ends of model Holliday Junction oligonucleotides. Finally, we have identified several components of the double-stranded break repair machinery that strongly interact with hMSH4-hMSH5. These results further underline the function (s) and interactors of hMSH4-hMSH5 that ensure accurate chromosomal repair and segregation during meiosis.

MutS homologs (MSH) [2] have been identified in most organisms examined. Bacteria may contain one or two MSH proteins, whereas the yeast *Saccharomyces cerevisiae* has been found to contain six MSH proteins (MSH1–MSH6), five of which are conserved in human (hMSH2–hMSH6) (for review see Refs. 1 and 2). MSH proteins appear to perform specific function(s) in mismatch repair (MSH2, MSH3, and MSH6) and meiosis (MSH4 and MSH5).

The *Escherichia coli* MutS functions as an asymmetric homodimer. This fundamental asymmetric nature appears conserved in the five human MSH proteins that form three heterodimers, hMSH2-hMSH3, hMSH2-hMSH6, and MSH4-MSH5 (3–5). The mismatch

*This work was supported by National Research Service Award T32-CA09662 and National Institutes of Health Grants CA67007 and GM62556. The costs of publication of this article were defrayed in part by the payment of page charges. This article must therefore be hereby marked "*advertisement*" in accordance with 18 U.S.C. Section 1734 solely to indicate this fact.

1To whom correspondence should be addressed: Wiseman 485N, 400 W. 12th Ave., Columbus, OH 43210. Tel.: 614-292-2484; rfishel@osu.edu.

[2]The abbreviations used are: MSH, MutS homologs; IVTT, *in vitro* transcribed/translated; DSB, double-strand break; HoJo, Holiday Junction; MMR, mismatch repair; GST, glutathione *S*-transferase; ATPγS, adenosine 5′-*O*-(thiotriphosphate); dsDNA, double-stranded DNA; EB, end blocked.

repair (MMR)-specific heterodimers hMSH2-hMSH3 and hMSH2-hMSH6 contain two interaction domains, one near the N terminus and one at the C terminus (5). These appear to generally correspond with hinge (C-terminal) and clasp (N-terminal) domains (5) that were confirmed in crystal structures of bacterial MutS bound to a mismatch (6,7). Whether similar peptide interaction region(s) exist between MSH4 and MSH5 are unknown.

MSH proteins belong to the Walker A/B family of ATPases (8,9). Extensive biochemical studies on the MMR-related MSH heterodimers have elucidated a highly conserved mechanism for mismatch recognition that is initiated by mismatched DNA provoked ADP → ATP exchange (10–12). Binding of ATP induces a conformational transition of the MSH dimer/heterodimer that results in the formation of a hydrolysis independent sliding clamp that is released from the mismatch and is free to diffuse along the adjacent duplex (10,13). Iterative rounds of mispair binding and ADP → ATP exchange appear to load multiple ATP-bound MSH sliding clamps that not only mark the mismatch region, but are also capable of interacting with specific downstream factors to effect repair and/or apoptosis (10,13,14).

MSH4 and MSH5 appear to be uniquely expressed in the testis and ovaries during prophase I of meiosis (4,15,16). Genetic studies in *S. cerevisiae*, *Caenorhabditis elegans*, *Arabidopsis thaliana*, and *Mus musculus* suggest that MSH4 and MSH5 are not involved in MMR but are required for normal chromosomal segregation and the production of viable gametes during meiosis (17–25). Both MSH4 and MSH5 affect the number and distribution of crossovers during meiosis, which suggests a role in both recombination and crossover interference (21, 26,27).

Pairing and synapsis of homologous chromosomes is an essential feature of meiosis I that results in genetic recombination and ensures accurate segregation of homologs (for review, see Ref. 28). The Holliday Junction (HoJo) was initially proposed as an intermediate in meiotic recombination that could account for both crossovers and gene conversion products (29). The double-strand break (DSB) repair model of recombination, which included tandem double Holliday Junctions (dHoJo) was later proposed to account for differences between the predicted and observed recombination products following meiosis (30). Such dHoJo's have been observed *in vivo* during meiosis in yeast (31).

Our previous studies established that hMSH4-hMSH5 uniquely and specifically recognizes a HoJo and its developmental precursor (32). We demonstrated that binding of hMSH4-hMSH5 to HoJo's provoked ADP → ATP exchange. ATP binding induced a conformational transition in the hMSH4-hMSH5 complex that resulted in a hydrolysis-independent sliding clamp, which dissociated from the HoJo cross-over core embracing two stacked parental duplex arms adjacent to the crossover. These observations led us to propose that hMSH4-hMSH5 stabilized and preserved the meiosis I HoJo intermediate until it was appropriately resolved to ensure accurate parental chromosome segregation (32).

Here we have demonstrated that the hMSH4-hMSH5 heterodimer displays two interaction domains within each subunit located near the amino and at the C-terminal regions of the proteins that flank the adenosine nucleotide-binding domain. We show that both the hMSH4 and hMSH5 subunits bind ATP and the poorly hydrolysable analog of ATP, ATPγS. The collective binding of ATP by the individual subunits appears to account for the apparent $K_{D(ATP)}$ of the heterodimer. We also explore the mechanism of ADP → ATP exchange and determined that it occurs during recognition of the HoJo core. Hydrolysis of ATP does not occur until the ATP-bound hMSH4-hMSH5 sliding clamp transits the ends of the HoJo. Finally, we have identified several components of the DSB repair machinery that strongly interact with hMSH4 and/or hMSH5, suggesting components of both early and late

recombination nodules that may function with the hMSH4-hMSH5 heterodimer to ensure accurate DSB repair and chromosome segregation during meiosis I.

EXPERIMENTAL METHODS

Protein Purification

The overexpression and purification of hMSH4 and C-terminal His_6-tagged hMSH5 were performed as previously described (32). Protein concentrations were determined by Bradford analysis using gel filtration standards (Bio-Rad).

GST-IVTT Protein Interaction Assay

Preparation of GST-tagged protein lysates, *in vitro* transcription-translation (IVTT), and the GST-IVTT interaction assay were performed as previously described (33,34). Quantitation of each GST-IVTT interaction (Int_{rel}) was calculated based upon the number of [^{35}S]Met present in each IVTT product as described previously (35) using the interaction between full-length hMSH4-hMSH5 as the interaction standard. Previous studies have suggested that $Int_{rel} > 20\%$ may be considered significant. hMSH4 and hMSH5 truncations were constructed by PCR truncation mutagenesis. The hMSH4 forward primers contained the following sequence in addition to sequences complementary to the N-terminal truncation region of hMSH4: 5′-GGCTCTAGAATG-3′ (XbaI site). The hMSH4 reverse primers contained the following sequence in addition to sequences complementary to the C-terminal truncation region of hMSH4: 5′-CGGGGTACCTCA-3′ (KpnI site). These forward and reverse primers were used in a PCR with pET29a-hMSH4 as a template. The hMSH4 PCR product and pET29a were digested with XbaI and KpnI, gel purified, ligated, and subclones sequenced to assure validity. hMSH5 forward primers contained the following sequence in addition to sequences complementary to the N-terminal truncation region of hMSH5: 5′-GGAATTCCATATG-3′ (NdeI site). hMSH5 reverse primers contained the following sequence in addition to sequences complementary to the C-terminal truncation region of hMSH5: 5′-GGCATACTCGAGTCA-3′ (XhoI site). These forward and reverse primers were used in a PCR with pET29a-hMSH5 as a template. The hMSH5 PCR product and pET29a were digested with NdeI and XhoI, gel purified, ligated, and subclones sequenced to assure validity. For the hMSH5 internal deletion (del 289–530) hMSH5-pET29a was digested with AatII, gel purified, ligated, and subclones sequenced to assure validity.

Adenosine Nucleotide Cross-linking

Cross-linking of labeled adenosine nucleotide (α-^{32}P, γ-^{32}P, or γ-^{35}S) was performed in 10 μl of Buffer A(25m_MHepes pH 8.1, 100m_MNaCl, 5m_M $MgCl_2$, 1 m_M dithiothreitol, 5% glycerol, and 300 n_M protein) and incubated at 25 °C for 10 min. The samples were then transferred to ice and irradiated for 5 mm in a UV Stratalinker 1800 (Stratagene). An equal volume of 2 × loading buffer was added to each sample, followed by boiling for 5 min. The products of each reaction were then resolved on a 10% SDS-PAGE gel. Prior to drying, gels were stained with Coomassie Blue to ensure equivalent loading between lanes. Gels were dried and quantitated by PhosphorImager (GE Healthcare). Quantitation was determined as a relative ratio to hMSH5 density.

DNA Substrate Preparation

All oligonucleotides were synthesized by Midland Certified Reagent Company Inc. (Midland, TX). The dsDNA, YoJo, HoJo, 1EB-HoJo, and 2EB-HoJo substrates were annealed and purified as previously described (32). The Frayed-YoJo was prepared by annealing AXdt4O: 5′-
CTAGTATAGAGCCGGCGCGCCATGTCTAGATAGCGTTAGGTTTTTTTTTTTTTTT

TTTTTTTTTTTTTTTTTTTTTTT-3′ and KBdt4O: 5′-TTTTTTTTTTTTTTTTTTTTTTTTTTTTTTTTTTTTTTTCCTAACGCTATCTAGACATGGCGCGCCGGCTCTATACTAG-3′. All annealed DNA substrates were purified by high pressure liquid chromatography with a Gen-Pak-FAX column (Waters) and concentrated with Centricon columns (Amicon). When oligonucleotides carried a biotin group, it was linked to the 3′ end.

Steady-state ATPase and ADP → ATP Exchange

Steady-state ATPase assays were performed in Buffer B (25 mM Hepes pH 7.8, 100 mM NaC1, 1 mM dithiothreitol, 5 mM $MgC1_2$, 5% glycerol, and 50 μg/ml acetylated bovine serum albumin) and incubated at 25 °C for 30 min as previously described (11). ADP → ATP exchange assays were performed in Buffer B. Four different concentrations of hMSH4-hMSH5 (0.5, 1, 1.5, and 2 pmol) were incubated with 2.3 μM [^{3}H]ADP at 25 °C for 10 min. A 3-fold excess of DNA was then added to the reaction, and incubation continued for an additional 10 min, followed by the addition of 500 μM unlabeled ATP to start the reaction ($t = 0$). The reaction was stopped at the indicated time points by the addition of 4 ml of ice-cold stop buffer (25 mM Hepes pH 7.8, 100mM NaCl, 10mM $MgC1_2$, and 500 μg/ml acetylated bovine serum albumin), immediately filtered through a Millipore HAWP nitrocellulose membrane, washed with an additional 4 ml of stop buffer, the filters air-dried, and quantitated as previously described (11).

RESULTS

The Interaction Regions between hMSH4 and hMSH5

The human MMR-specific MSH heterodimers contain defined interaction regions that correlate with hinge and clasp domains identified in structural studies of bacterial MutS (5–7). To map interaction domains, a full-length GST fusion protein of hMSH4 or hMSH5 was incubated with [^{35}S]Met-labeled IVTT fragments of hMSH5 or hMSH4, respectively. Interactions may be compared in this system by using excess GST “bait” with limiting IVTT “prey”; where the each prey was introduced in a calculated equimolar concentration as determined from PhosphorImager quantitation of [^{35}S]Met-labeled IVTT protein and proportional to the number of methionine residues in each peptide fragment. Quantitation was displayed relative to the known interactions between full-length hMSH4 and hMSH5 (Int_{rel}) (for description, see Ref. 35). We demonstrate that full-length hMSH4 interacts strongly with hMSH5 either as an IVTT-hMSH4 with GST-hMSH5 (Fig. 1*A*, *lane 1*) or a GST-hMSH4 with IVTT-hMSH5 (Fig. 1*B*, *lane 1*). These two interactions represent an Int_{rel} of 100% for comparison to subsequent peptide interactions.

To determine the interaction regions of hMSH4 required for stable heterodimer formation with hMSH5 we first tested two overlapping truncated forms of hMSH4 (Fig. 1*A*, deletions, *lanes 2* and *6*). These studies suggested that both fragments interacted with full-length GST-hMSH5 (see Int_{rel} quantitation). Based upon these results, we constructed five additional deletions that truncated the interacting fragments del2 and del6. Three of these fragments (del4, −5, and −8) displayed little or no interaction with GST-hMSH5 (Fig. 1*A*, deletions, *lanes 4*, *5*, and *8*). In contrast, two fragments (del3 and del7) displayed significant interaction with full-length GST-hMSH5 (Fig. 1*A*, deletions, *lanes 3* and *7*). Taken as a whole these studies suggest two interaction regions, one near the N-terminal region (amino acids 357– 462) and one at the C-terminal region (amino acids 786 –936).

To determine the interaction regions of hMSH5 with hMSH4, IVTT truncation fragments of hMSH5 were tested for their ability to interact with full-length GST-hMSH4. Initially we examined three overlapping truncated forms of hMSH5 (Fig. 1*B*, deletions, *lanes 2*, *8*, and *9*).

We found that two of these (deletions, *lane 2* and *9*) significantly interacted with full-length GST-MSH4 (Fig. 1*B*, see Int_{rel} quantitation). Further truncating del9 (Fig. 1*B*, *del10*) resulted in a strong interaction. These results suggest an interaction region between amino acids 784 and 834 of hMSH5 with hMSH4. We subdivided del2 into four overlapping fragments (del3, -4, -5, and -6) and observed a strong interaction with del4 and del5 and little or no interaction with del3 and del6 (Fig. 1*B*, deletions, *lanes 3–6*). These results were most consistent with an interaction region between amino acids 152 and 263 of hMSH5 with hMSH4. The lack of any interaction with del3 is possibly a result of peptide misfolding: an inconvenient problem sometime associated with the IVTT-GST system. As a confirmation of these interaction motifs we constructed del7 containing both the N-terminal and C-terminal interaction regions with a deletion of an internal region between amino acids 270 and 558. We found a significant interaction with full-length GST-hMSH4 (Fig. 1*B*, deletion, *lane 7*). Overall, these results suggest that hMSH4 and hMSH5 interact in two distinct regions that flank the Walker A/B nucleotide-binding domain (Fig. 1*C*). These results appear qualitatively similar to the hinge and clasp domains identified in MMR-specific proteins hMSH2, hMSH3, and hMSH6 (5) that were largely confirmed following structural analysis of bacterial MutS (6,7).

Both Subunits of the hMSH4-hMSH5 Heterodimer Bind Adenosine Nucleotide

hMSH4 and hMSH5 both contain a consensus Walker A/B nucleotide-binding domain. Our previous studies demonstrated ADP ($K_{D(ADP)} \approx 20\ \mu M$) and ATPγS ($K_{D(ATP\gamma S)} \approx 5.9\ \mu M$) binding activity as well as HoJo-stimulated ATPase activity by the hMSH4-hMSH5 heterodimer (32). To examine ATP binding by individual hMSH4-hMSH5 subunits we performed UV cross-linking studies with [α-^{32}P]ATP, [γ-^{32}P]ATP, and [γ-^{35}S]ATP (Fig. 2).

We observed non-equivalent cross-link labeling of the hMSH4 and hMSH5 subunits when [α-^{32}P]ATP and [γ-^{32}P]ATP were used as substrates (Fig. 2, *A* and *B*). Whereas hMSH5 was efficiently cross-link labeled with [α-^{32}P]ATP and [γ-^{32}P]ATP at the lowest concentrations of adenosine nucleotide (160 nM), the hMSH4subunits only became efficiently labeled at higher concentrations ($c_{1/2} \approx 500$ nM).[3] Although inefficient, both subunits appeared to be cross-link labeled equivalently over the entire range of [γ-^{35}S]ATP concentrations (Fig. 2*C*). We observe no difference in UV cross-linking in the presence or absence of Holliday Junction DNA (Fig. 2*E*). This variation in cross-linking efficiency may suggest different binding properties or perhaps unique orientation(s) of the adenosine nucleotide in the binding region that affect cross-link efficiency.

Because the cross-linking was performed at adenosine nucleotide concentrations that were well below the K_D for ATP/ATPγS, we performed competition analysis with unlabeled ATP (Fig. 3). In these studies, unlabeled ATP was added to the labeled adenosine nucleotide prior to cross-linking. We observed equivalent competition by individual hMSH4 and hMSH5 subunits cross-linked with [α-^{32}P]ATP ($K_{I(ATP)} \approx 4\ \mu M$) and [γ-^{35}S]ATP ($K_{I(ATP)} \approx 12\ \mu M$) (Fig. 3, *A* and *C*). The average of these results correlate well with the observed K_D for ATPγS determined by filter binding (32). We found a differential competition for cross-linking of hMSH4 and hMSH5 with [γ-^{32}P]ATP (hMSH4 $K_{I(ATP)} \approx 4\ \mu M$; hMSH5 $K_{I(ATP)} \approx 12 \mu M$;Fig. 3*B*). The increase in $K_{I(ATP)}$ of hMSH5 observed when cross-linked with [α-^{32}P]ATP compared with [γ-^{32}P]ATP most likely reflects subunit ATP processing. In the case of [α-^{32}P]ATP, the cross-linked adenosine residue may be ATP, ADP, or a mixture of these adenosine nucleotides. However, competition of cross-linked [γ-^{32}P]ATP must *a priori* reflect ATP competition. Taken as a whole, these results suggest an asymmetry in ATP binding and/or hydrolysis by individual subunits: an observation that is consistent with other MSH dimers/heterodimers (36).

[3] $c_{1/2}$ is defined as the concentration of labeled ATP, which produces half the total labeling.

hMSH4-hMSH5 ATPase and ADP → ATP Exchange Is Uniquely Stimulated by Holliday Junctions

DNA containing mismatches display differential specificity in the stimulation of the intrinsic ATPase activity of MMR-specific MSH proteins (11,13,37–39). We examined the specificity of the hMSH4-hMSH5 steady-state ATPase activity. The hMSH4-hMSH5 ATPase was stimulated by HoJo's or a HoJo precursor (Pro-HoJo) containing three duplex arms and a single-stranded arm surrounding the crossover region (32) (Fig. 4*A*). Our previous studies suggested little or no binding to a three-way junction (Y-Junction or YoJo), although its ability to stimulate the intrinsic ATPase was unknown. We observed a slight stimulation of the hMSH4-hMSH5 ATPase in the presence of dsDNA, YoJo, or Frayed-YoJo DNAs compared with the absence of DNA (Fig. 4*A*). This modest ATPase stimulation by canonical dsDNA has been observed with MMR-specific MSH proteins and has been interpreted to be the result of nonspecific DNA end stimulation (10,11,40).

ADP → ATP exchange has been shown to be the rate-limiting step for the intrinsic steady-state ATPase of bacterial and eukaryotic MSH proteins (10–12). The kinetics of ADP → ATP exchange may be examined by prebinding hMSH4-hMSH5 with [^{3}H]ADP in the presence of Mg^{2+}. The ADP → ATP exchange reaction is started by the addition of excess unlabeled ATP in the presence or absence of a DNA substrate. Our previous studies demonstrated that hMSH4-hMSH5 ADP → ATP exchange was stimulated by HoJo and pro-HoJo DNA substrates (32) (Fig. 4*B*). HoJo-dependent ADP release required the addition of exogenous ATP indicating a *bona fide* ADP → ATP exchange process (32) (data not shown). As reported previously, little or no ADP → ATP exchange was observed in the absence of DNA or in the presence of dsDNA providing continued controls for the analysis (32) (Fig. 4*B*).

We examined the ability of the YoJo or a Y-Junction containing one duplex and two single-stranded 40-mer arms (Frayed-YoJo) (Fig. 4*B*). Both structures were found to produce a slight stimulation of ADP → ATP exchange compared with the absence of DNA, although there was no significant difference when compared with dsDNA. These latter results are qualitatively similar to MMR-specific MSH proteins and like the ATPase, have been interpreted to be the result of nonspecific DNA end stimulation (10). By comparison, HoJo DNA provokes rapid and extensive ADP → ATP exchange as we have shown previously (32). Taken with the ATPase data, these observations place important limits on the types of DNA structures that provoke ATP processing by hMSH4-hMSH5; suggesting high specificity for HoJo and pro-HoJo structures (see Ref. 1 for pro-HoJo studies).

Stimulation of hMSH4-hMSH5 ATPase but Not ADP → ATP Exchange Requires an Open-end Holliday Junction

Previous studies with MMR-specific MSH proteins have led to the hypothesis that ATP hydrolysis largely occurs following transit off the DNA ends of model oligonucleotides (10, 13,32). Importantly, ATP-bound hydrolysis-independent sliding clamps may be trapped on these same model oligonucleotides by blocking the ends with biotin-streptavidin; with consequent reduction of ATPase activity (10,13,32). We constructed a HoJo substrate that contained biotin on all four DNA ends (*b*-HoJo). Previous studies showed that addition of streptavidin to *b*-HoJo DNA blocked the release of hMSH4-hMSH5 in the presence of ATP (32). One unpublished formal possibility was that in the presence of streptavidin the *b*-HoJo inhibited ADP release and/or ATP binding by hMSH4-hMSH5. We found that the *b*-HoJo-stimulated ADP → ATP exchange was similar to the unbiotinylated HoJo (compare Fig. 5*A* with 4*A*) and that streptavidin alone had no catalytic effect on ADP → ATP exchange (Fig. 5*A*). Interestingly, the addition of streptavidin to *b*-HoJo DNA provoked a similar stimulation of hMSH4-hMSH5 ADP → ATP exchange as the *b*-HoJo or the nonbiotinylated HoJo DNAs (compare Fig. 5*A* and 4*A*). These results are consistent with the conclusion that blocking the

ends of the HoJo DNA substrate does not affect its ability to provoke hMSH4-hMSH5 ADP → ATP exchange (32).

We determined that the *b*-HoJo or the unbiotinylated HoJo in the presence of streptavidin, stimulated the hMSH4-hMSH5 ATPase similar to the HoJo alone (compare Fig. 5*B* with 4*B*). However, the addition of streptavidin to the *b*-HoJo dramatically decreased the hMSH4-hMSH5 ATPase (Fig. 5*B*). These results appear qualitatively similar to the reduction in ATPase observed with blocked-end mismatched substrates and MMR-specific MSH proteins. Taken as a whole, we conclude that hMSH4-hMSH5 steady-state ATP hydrolysis requires unblocked HoJo DNA.

Work by Lilly and colleagues (41) have demonstrated that the four arms of a HoJo adopt a "stacked-X" configuration. Our previous work showed that blocking one of the two arms on *both* ends of the stacked-X (2EB) was sufficient to retain hMSH4-hMSH5 on a HoJo (32). These results were interpreted to suggest hMSH4-hMSH5 formed a hydrolysis-independent sliding clamp that embraced two duplex arms of a HoJo (32).

The hMSH4-hMSH5 ATPase studies were consistent with two possibilities: 1) any single open-end on a HoJo DNA is capable of provoking hMSH4-hMSH5 ATP hydrolysis, or 2) transit of hMSH4-hMSH5 off the openend(s) of a HoJo is required for ATP hydrolysis. The 2EB HoJo appeared to be a superb substrate to distinguish between these two possibilities because each side of a stacked-X contains one blocked-end and one open-end. Whereas the 2EB HoJo structure was capable of retaining hMSH4-hMSH5 sliding clamps, the ability of these half-blocked end structures to provoke ADP → ATP exchange has not been reported. We found that 2EB as well as a HoJo containing a single (one of four) biotin-stretavidin blocked end (1EB) provoked hMSH4-hMSH5 ADP → ATP exchange equivalently to an unblocked HoJo (Fig. 6*A*). We conclude that HoJo-dependent ADP release and subsequent ATP binding is unaffected by blocking any of the four DNA ends with biotin-streptavidin.

We examined these same substrates for their ability to stimulate the hMSH4-hMSH5 ATPase activity (Fig. 6*B*). We also observed no stimulation of the hMSH4-hMSH5 ATPase in the presence of streptavidin alone when compared with the absence of DNA (data not shown; Fig. 4*A*). Moreover, an unblocked HoJo or the 1EB HoJo appeared to stimulate the hMSH4-hMSH5 ATPase activity equivalently (k_{cat}/K_m = 0.0016 min^{-1} μM^{-1}, K_m = 125 μM; k_{cat}/K_m = 0.0014 min^{-1} μM^{-1}, K_m = 132 μM, respectively). However, the 2EB HoJo DNA drastically reduced the hMSH4-hMSH5 ATPase activity to levels observed in the absence of DNA (k_{cat}/K_m = 0.004 min^{-1} μM^{-1}, K_m = 193 μM; Fig. 6*B*). These results are consistent with the conclusion that an open-end DNA is not sufficient to provoke hMSH4-hMSH5 ATP hydrolysis; rather ATP hydrolysis requires transit off the stacked HoJo ends.

hMSH4-hMSH5 Interacts with a Subset of Recombination Proteins

The pairing of homologous chromosomes prior to the reduction division associated with meiosis I is accomplished by DSB repair of hundreds of induced chromosomal DSBs (42, 43). Our previous studies have suggested that hMSH4-hMSH5 recognizes the recombination intermediates of pro-HoJo and HoJo associated with DSB repair (32). The formation of these pro-HoJo and HoJo structures requires a number of recombination components that include the RecA/RAD51 family members. We surveyed several human recombination components for their interaction with hMSH4 and hMSH5 using the GST-IVTT interaction methodology. Interactions were quantified relative to the known stable interaction between hMSH4 and hMSH5 ($Int_{rel(hMSH4)}$ or $Int_{rel(hMSH5)}$; Fig. 7).

We found a specific interaction between hMSH4 and human RecA/RAD51 family members hRAD5ID and XRCC3 (Fig. 7*A*). In addition, hMSH4 appears to strongly interact with the

recombination SWI/SNF helicase hRAD54 (Fig. 7*A*). The interaction between hMSH4 and hXRCC3 appears to be nearly twice as robust as the interaction between hMSH4and hMSH5. We observed a similar strong interaction between hMSH5 and hRAD51D, hXRCC3, and hRAD54; the latter nearly twice the stable interaction between hMSH4 and hMSH5 (Fig. 7*B*). We also observed a specific interaction between hMSH5 and hRAD51B ($Int_{rel(hMSH4)}$ = 58%; Fig. 7*B*), whereas the interaction between hMSH4 and hRAD51B was significantly less robust ($Int_{rel(hMSH5)}$ = 23%; Fig. 7*A*). No significant observed interaction was observed between either hMSH4 or hMSH5 with hRad51, hRAD51C, hXRCC2, and hRAD52. The lack of a direct interaction between hMSH4 and hRAD51 contrasts to the report of Neyton *et al.* (44). We have also observed a modest interaction between hMSH4 and hMSH5 with hExol (data not shown), an exonuclease thought to be involved in recombination intermediate processing during meiosis (45). These studies begin to detail the individual interactions between protein components that appear in the recombination foci during meiosis I.

DISCUSSION

We initially demonstrated that hMSH4 and hMSH5 formed a specific heterodimer similar to other MSH proteins (4). These studies laid the foundation for mapping the interaction regions between the hMSH4 and hMSH5 heterodimer. Our results indicate that much like the hMSH2-hMSH3 and hMSH2-hMSH6 complexes, hMSH4 and hMSH5 interact in two regions between subunits that flank the consensus adenosine nucleotide-binding domain (Fig. 1). These two regions would appear to correspond to the hinge and clasp domains originally proposed by Guerrette *et al.* (5) and confirmed in the crystal structures of *Thermus aquaticus* and *E. coli* MutS (6,7). Based on sequence alignment, it has been proposed that the MSH4-MSH5 heterodimer contains a large centrally located interior hole (30 Å × 70 Å), due in part to the absence of a mismatch-interrogation domain (Domain I) (7). Our interaction analysis would appear to support this conclusion. Combined with our proposal that ATP-bound hMSH4-hMSH5 forms a sliding clamp that embraces stacked duplex arms of a HoJo (32), it is intriguing to visualize two duplex DNA arms resting in this large interior hole.

We found that the hMSH4-hMSH5 heterodimer contains an intrinsic HoJo-stimulated ATPase (32). Yet, it was unclear whether one or both subunits of the heterodimer were involved in processing ATP. Our adenosine nucleotide cross-linking studies suggest that both hMSH4 and hMSH5 bind [α-^{32}P]ATP, [γ-^{32}P]ATP, and [γ-^{35}S]ATP (Fig. 2). Furthermore, the ATP binding activity derived from competition analysis (average $K_{D(ATP)} \approx 6$ μM) appeared similar to our previously published ATP binding activity derived from filter binding studies ($K_{D(ATP)} \approx 5.9$ μM). Cross-linking with [γ-^{35}S]ATP was exceedingly inefficient and may reflect an altered orientation of the cross-linkable adenosine residue associated with the placement of a ^{35}S-moiety on the γ-phosphate. Interestingly, the hMSH4 subunit appears to display reduced [γ-^{32}P]ATP and [γ-^{32}P]ATP cross-linking ($c_{1/2} \approx 400$ nM) compared with the hMSH5 subunit ($c_{1/2} \ll 160$ nM) at sub-K_D concentrations of adenosine nucleotide (Fig. 2). A similar subunit difference was noted in ATP competition studies for [γ-^{32}P]ATP cross-linking (Fig. 3). These results support the hypothesis that hMSH4 and hMSH5 contain asymmetric ATP processing activities; an observation that is consistent with all previously studied MSH dimers/heterodimers.

Analysis of the hMSH4-hMSH5 steady-state ATPase and ADP → ATP exchange activities suggests unique activation by HoJo and pro-HoJo DNA structures. These results are consistent with previous DNA binding studies (32). hMSH4-hMSH5 does not recognize and is not activated by single-stranded DNA, dsDNA, YoJo DNA, or frayed-YoJo DNA (Fig. 4). This observation places significant limits on the type of DNA structure that is recognized and subsequently activates ADP → ATP exchange by the hMSH4-hMSH5 heterodimer.

Our studies strongly supported the hypothesis that it is the recognition of HoJo and pro-HoJo core DNA crossover regions that provokes ADP → ATP exchange by hMSH4-hMSH5. The observation of ADP → ATP exchange with blocked-end HoJo DNA further substantiates this conclusion (Fig. 4– Figs. 6). In contrast, the steady-state ATPase appears dramatically reduced in the presence of blocked-end HoJo DNA (Fig. 5). This latter result suggested that an open DNA end was required to trigger ATP hydrolysis. A similar conclusion has been forwarded for MMR-specific MSH proteins (10,13). The unique structure of HoJo DNAs allowed us to test whether it was the DNA end or transit off the DNA end that provoked hMSH4-hMSH5 ATP hydrolysis. The 2EB-HoJo DNA contains a single block on one of the two duplex ends on each side of the stacked-X HoJo arms. We have previously shown that 2EB-HoJo DNA retains ATP-bound hMSH4-hMSH5 sliding clamps, which is the basis of the proposal that hMSH4-hMSH5 forms a sliding clamp that embraces two duplex arms of a stacked-X HoJo DNA (32). The hMSH4-hMSH5 ATPase activity in the presence of 2EB-HoJo appeared similar to the background activity in the absence of DNA or in the presence of dsDNA. These results appear to significantly reduce the possibility that interaction with the DNA end stimulates the hMSH4-hMSH5 ATPase. Rather it appears more likely that transit off the HoJo DNA end is required to stimulate the hMSH4-hMSH5 ATPase. We regard it similarly likely that all other MSH ATPase activities are stimulated by transit off the model oligonucleotide structures for which they show specific binding/activation activity.

The central role of hMSH4 and hMSH5 in meiosis I recombination and chromosome segregation suggested interaction(s) with other DSB repair components. Using a simple *in vitro* GST/IVTT methodology, we have identified specific interaction(s) between hMSH4 and hMSH5 with the RecA/RAD51 family members hRAD51D and XRCC3 (Fig. 7). hMSH5 also appears to significantly interact with hRAD51B. In the case of hXRCC3, the relative interaction with hMSH4 and hMSH5 was nearly twice that of the interaction between the known hMSH4-hMSH5 heterodimer (Fig. 7). The role of XRCC3 in DSB repair is unknown. The hRAD51C-XRCC3 heterodimer has been suggested to contain a Holliday resolvase activity (46,47). Importantly, RAD51C knock-out mice display a meiosis I pachytene arrest phenotype that appears largely similar to hMSH4 and hMSH5 knock-out mice (48). We find no significant interaction between hMSH4 or hMSH5 with hRAD51 unlike a previous report (Fig. 7) (44). These results appear to suggest that hMSH4-hMSH5 interacts with one or several of the reported hRAD51-paralog higher order complexes, rather than directly with hRAD51 or the hRAD51 nucleoprotein filament that encourages homologous recombination during meiosis I.

Both hMSH4 and hMSH5 strongly interact with hRAD54 (Fig. 7). The RAD54 SWI/SNF helicase appears to enhance hRAD51 strand exchange by stabilizing the hRAD51 nucleo-protein filament (49,50). The biochemical function of the hRAD54-hMSH4-hMSH5 interaction is unknown. One of the deficiencies in this and previous reports describing meiotic protein associations is the lack of useful meiotic tissues to verify protein interactions.

We have proposed a role for hMSH4-hMSH5 in stabilizing pro-HoJo and HoJo DNA structures during meiosis I homologous recombination (32). The results presented here further support and extend this model. Both hMSH4 and hMSH5 appear to play additional role(s) in genetic interference (21,22,24,25); a century old observation that suggests a single crossover interferes with the development of nearby crossovers (51,52). Crossover interference may extend for megabases on either side of the known crossover. Of the ~400 DSBs introduced during the development of mammalian germ cells, the vast majority (~90%) are resolved by non-crossover events. The biochemical role of hMSH4-hMSH5 in preserving crossovers and driving nearby recombination events into non-crossovers is unknown. This process is complicated by the observation that hMSH4-hMSH5 foci appear to form on all DSB repair events, but are only found in late pachytene on chiasmata/crossovers (53), which are also marked by hMLH1-

hMLH3 (54,55). These observations suggest an active process in which hMSH4-hMSH5 sliding clamps are removed from DSB repair structures destined for non-crossovers, whereas they are retained on DSB repair structures destined for crossovers. To date, the hMSH4-hMSH5 heterodimer is the only known protein complex that is retained during this genetic transition. It is worth noting that our observed interaction between hMSH4 and hMSH5 with hRAD54 combined with reports that RAD54 may translocate on DNA for distances of up to 30 kb (56) may have some mechanistic relevance to genetic interference. Further studies will be required to understand the biochemical process(es) that provide the basis for genetic interference.

Acknowledgments

We thank Kristine Yoder for many helpful discussions and critical review and Chuck Butz for technical assistance.

REFERENCES

1. Eisen JA. Nucleic Acids Res 1998;26:4291–4300. [PubMed: 9722651]
2. Fishel R, Wilson T. Curr. Opin. Genet. Dev 1997;7:105–113. [PubMed: 9024626]
3. Acharya S, Wilson T, Gradia S, Kane MF, Guerrette S, Marsischky GT, Kolodner R, Fishel R. Proc. Natl. Acad. Sci. U. S. A 1996;93:13629–13634. [PubMed: 8942985]
4. Bocker T, Barusevicius A, Snowden T, Rasio D, Guerrette S, Robbins D, Schmidt C, Burczak J, Croce CM, Copeland T, Kovatich AJ, Fishel R. Cancer Res 1999;59:816–822. [PubMed: 10029069]
5. Guerrette S, Wilson T, Gradia S, Fishel R. Mol. Cell. Biol 1998;18:6616–6623. [PubMed: 9774676]
6. Lamers MH, Perrakis A, Enzlin JH, Winterwerp HH, de Wind N, Sixma TK. Nature 2000;407:711–717. [PubMed: 11048711]
7. Obmolova G, Ban C, Hsieh P, Yang W. Nature 2000;407:703–710. [PubMed: 11048710]
8. Fishel R. Genes Dev 1998;12:2096–2101. [PubMed: 9679053]
9. Walker JE, Saraste M, Runswick MJ, Gay NJ. EMBO J 1982;1:945–951. [PubMed: 6329717]
10. Acharya S, Foster PL, Brooks P, Fishel R. Mol. Cell 2003;12:233–246. [PubMed: 12887908]
11. Gradia S, Acharya S, Fishel R. Cell 1997;91:995–1005. [PubMed: 9428522]
12. Wilson T, Guerrette S, Fishel R. J. Biol. Chem 1999;274:21659–21664. [PubMed: 10419475]
13. Gradia S, Subramanian D, Wilson T, Acharya S, Makhov A, Griffith J, Fishel R. Mol. Cell 1999;3:255–261. [PubMed: 10078208]
14. Fishel R. Nat. Med 1999;5:1239–1241. [PubMed: 10545986]
15. Her C, Doggett NA. Genomics 1998;52:50–61. [PubMed: 9740671]
16. Moens PB, Kolas NK, Tarsounas M, Marcon E, Cohen PE, Spyropoulos B. J. Cell Sci 2002;115:1611–1622. [PubMed: 11950880]
17. de Vries SS, Baart EB, Dekker M, Siezen A, de Rooij DG, de Boer P, te Riele H. Genes Dev 1999;13:523–531. [PubMed: 10072381]
18. Edelmann W, Cohen PE, Kneitz B, Winand N, Lia M, Heyer J, Kolodner R, Pollard JW, Kucherlapati R. Nat. Genet 1999;21:123–127. [PubMed: 9916805]
19. Franklin FC, Higgins JD, Sanchez-Moran E, Armstrong SJ, Osman KE, Jackson N, Jones GH. Biochem. Soc. Trans 2006;34:542–544. [PubMed: 16856855]
20. Higgins JD, Armstrong SJ, Franklin FC, Jones GH. Genes Dev 2004;18:2557–2570. [PubMed: 15489296]
21. Hollingsworth NM, Ponte L, Halsey C. Genes Dev 1995;9:1728–1739. [PubMed: 7622037]
22. Kelly KO, Dernburg AF, Stanfield GM, Villeneuve AM. Genetics 2000;156:617–630. [PubMed: 11014811]
23. Kneitz B, Cohen PE, Avdievich E, Zhu L, Kane MF, Hou H Jr. Kolodner RD, Kucherlapati R, Pollard JW, Edelmann W. Genes Dev 2000;14:1085–1097. [PubMed: 10809667]
24. Ross-Macdonald P, Roeder GS. Cell 1994;79:1069–1080. [PubMed: 8001134]

25. Zalevsky J, MacQueen AJ, Duffy JB, Kemphues KJ, Villeneuve AM. Genetics 1999;153:1271–1283. [PubMed: 10545458]
26. Kolas NK, Cohen PE. Cytogenet. Genome Res 2004;107:216–231. [PubMed: 15467367]
27. Novak JE, Ross-Macdonald PB, Roeder GS. Genetics 2001;158:1013–1025. [PubMed: 11454751]
28. Roeder GS. Genes Dev 1997;11:2600–2621. [PubMed: 9334324]
29. Holliday RA. Genet. Res 1964;5:282–304.
30. Szostak JW, Orr-Weaver TL, Rothstein RJ, Stahl FW. Cell 1983;33:25–35. [PubMed: 6380756]
31. Allers T, Lichten M. Mol. Cell 2001;8:225–231. [PubMed: 11511375]
32. Snowden T, Acharya S, Butz C, Berardini M, Fishel R. Mol. Cell 2004;15:437–451. [PubMed: 15304223]
33. Bocker T, Ruschoff J, Fishel R. Biochim. Biophys. Acta 1999;31:O1–O10. [PubMed: 10382540]
34. Schmutte C, Sadoff MM, Shim KS, Acharya S, Fishel R. J. Biol. Chem 2001;276:33011–33018. [PubMed: 11427529]
35. Guerrette S, Acharya S, Fishel R. J. Biol. Chem 1999;274:6336–6341. [PubMed: 10037723]
36. Lamers MH, Winterwerp HH, Sixma TK. EMBO J 2003;22:746–756. [PubMed: 12554674]
37. Blackwell LJ, Bjornson KP, Modrich P. J. Biol. Chem 1998;273:32049–32054. [PubMed: 9822679]
38. Gradia S, Acharya S, Fishel R. J. Biol. Chem 2000;275:3922–3930. [PubMed: 10660545]
39. Haber LT, Walker GC. EMBO J 1991;10:2707–2715. [PubMed: 1651234]
40. Mazur DJ, Mendillo ML, Kolodner RD. Mol. Cell 2006;22:39–49. [PubMed: 16600868]
41. Duckett DR, Murchie AI, Diekmann S, von Kitzing E, Kemper B, Lilley DM. Cell 1988;55:79–89. [PubMed: 3167979]
42. Hassold T, Sherman S, Hunt P. Hum. Mol. Genet 2000;9:2409–2419. [PubMed: 11005796]
43. Kleckner N. Proc. Natl. Acad. Sci. U. S. A 1996;93:8167–8174. [PubMed: 8710842]
44. Neyton S, Lespinasse F, Moens PB, Paul R, Gaudray P, Paquis-Flucklinger V, Santucci-Darmanin S. Mol. Hum. Reprod 2004;10:917–924. [PubMed: 15489243]
45. Tran PT, Erdeniz N, Symington LS, Liskay RM. DNA Repair (Amst.) 2004;3:1549–1559. [PubMed: 15474417]
46. Liu Y, Masson JY, Shah R, O'Regan P, West SC. Science 2004;303:243–246. [PubMed: 14716019]
47. Liu Y, Tarsounas M, O'Regan P, West SC. J. Biol. Chem 2007;282:1973–1979. [PubMed: 17114795]
48. Kuznetsov S, Pellegrini M, Shuda K, Fernandez-Capetillo O, Liu Y, Martin BK, Burkett S, Southon E, Pati D, Tessarollo L, West SC, Donovan PJ, Nussenzweig A, Sharan SK. J. Cell Biol 2007;176:581–592. [PubMed: 17312021]
49. Mazin AV, Alexeev AA, Kowalczykowski SC. J. Biol. Chem 2003;278:14029–14036. [PubMed: 12566442]
50. Mazin AV, Bornarth CJ, Solinger JA, Heyer WD, Kowalczykowski SC. Mol. Cell 2000;6:583–592. [PubMed: 11030338]
51. Muller HJ. Am. Nat 1916;50:193–221.
52. Sturtevant AH. Z. Abstam. Vererbung 1915;13:234–287.
53. Lenzi ML, Smith J, Snowden T, Kim M, Fishel R, Poulos BK, Cohen PE. Am. J. Hum. Genet 2005;76:112–127. [PubMed: 15558497]
54. Kolas NK, Svetlanov A, Lenzi ML, Macaluso FP, Lipkin SM, Liskay RM, Greally J, Edelmann W, Cohen PE. J. Cell Biol 2005;171:447–458. [PubMed: 16260499]
55. Lipkin SM, Moens PB, Wang V, Lenzi M, Shanmugarajah D, Gilgeous A, Thomas J, Cheng J, Touchman JW, Green ED, Schwartzberg P, Collins FS, Cohen PE. Nat. Genet 2002;31:385–390. [PubMed: 12091911]
56. Heyer WD, Li X, Rolfsmeier M, Zhang XP. Nucleic Acids Res 2006;34:4115–4125. [PubMed: 16935872]

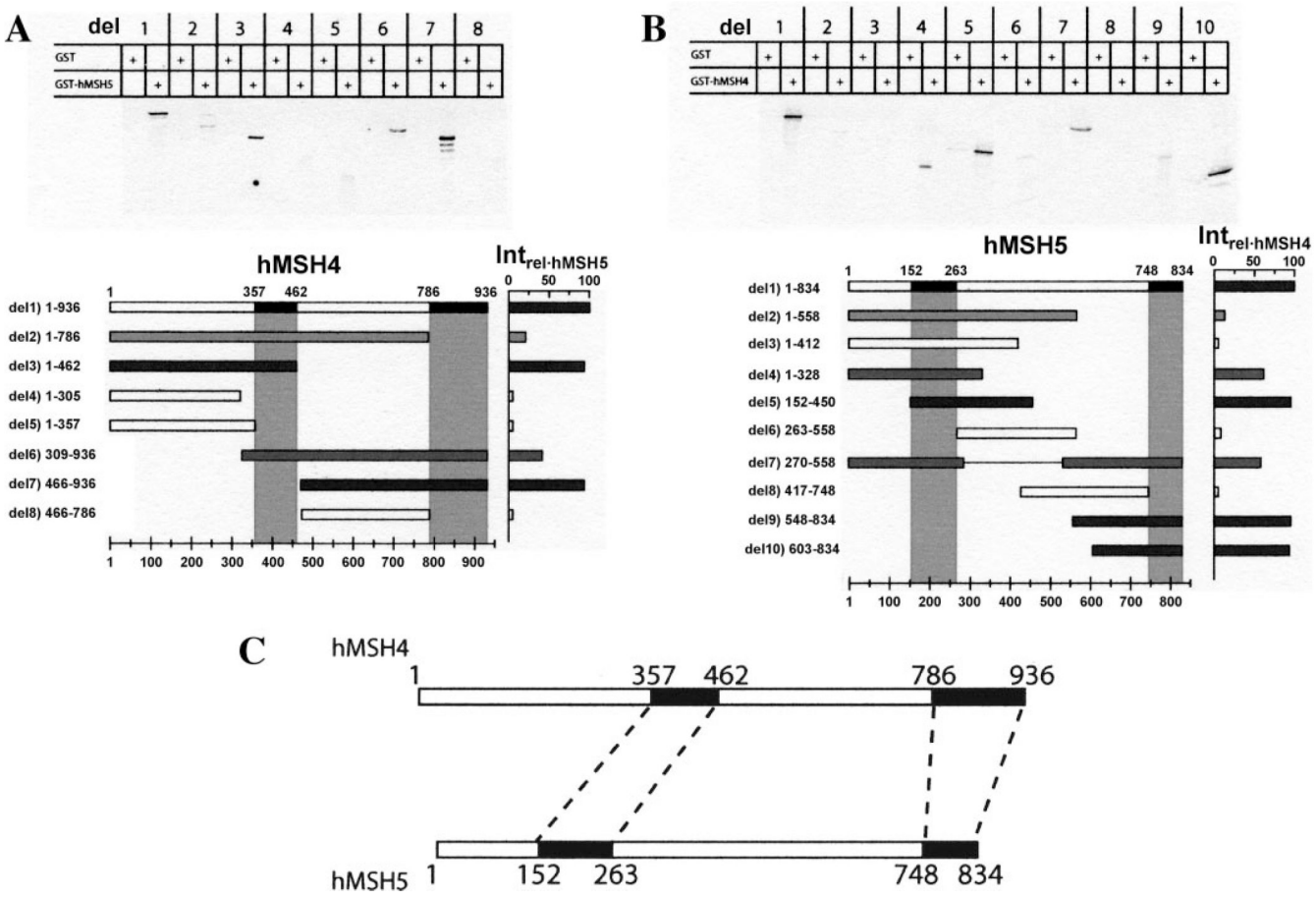

FIGURE 1. The interaction regions between hMSH4 and hMSH5

A, regions of hMSH4 required for interaction with hMSH5. *B*, regions of hMSH5 required for interaction with hMSH4. [^{35}S]Met-labeled full-length and truncation mutants of IVTT-hMSH4 (*A*) or truncation mutants of IVTT-hMSH5 (*B*) were incubated with glutathione beads prebound with either GST (alone) or full-length GST-hMSH5 (*A*) or full-length GST-hMSH4. Following processing, reactions were separated on a 10% SDS-PAGE gel and visualized by phosphorimager. Illustrations of the mutant constructs are shown *below* the gels on both panels. *Numbers* correspond to the individual numbered deletions (*del*) and the reaction separated by the gel above. The consensus interaction peptides are shown in the *shaded blue-gray* (Int_{rel} 20–75%) or *black* (Int_{rel} 75–100%) box. *C*, hMSH4-hMSH5 forms a specific heterodimer that contains two interaction regions. An illustration with the two interaction regions containing numbered amino acids is shown.

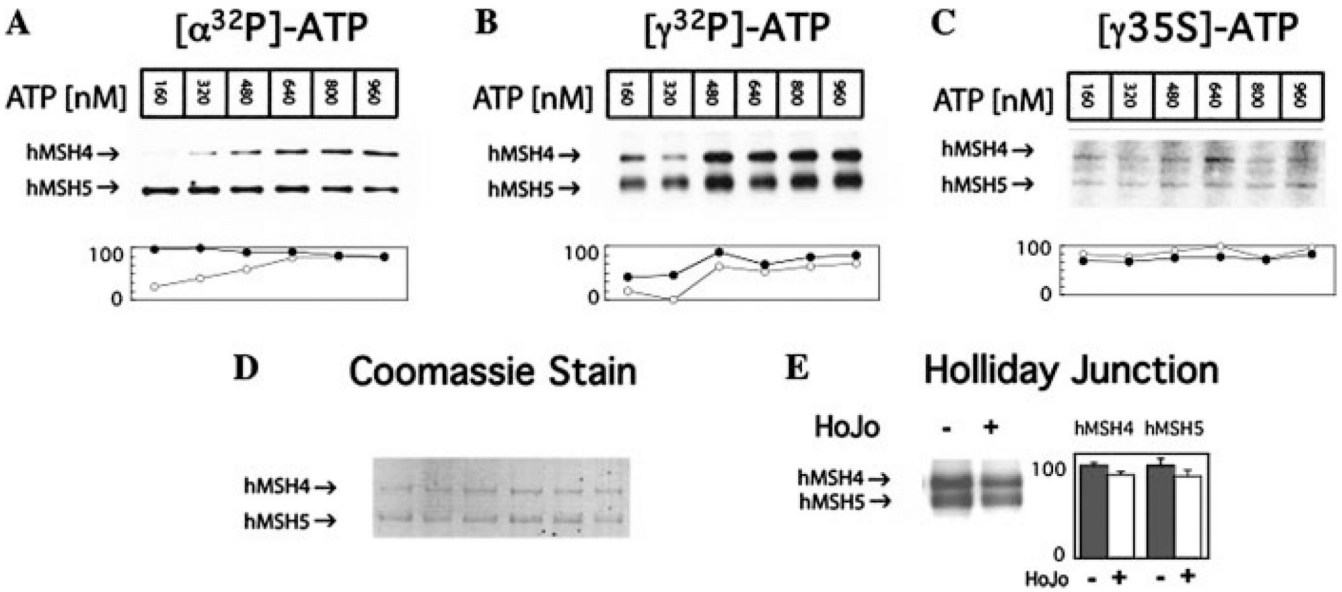

FIGURE 2. Both subunits of hMSH4-hMSH5 bind ATP and ATPγS

hMSH4-hMSH5 (100 nM) was incubated with the indicated concentrations of labeled ATP and exposed to UV cross-linking. Reactions were separated on a 10% SDS-PAGE gel and visualized via phosphorimager (shown *below each panel*). *A*, [α-^{32}P]ATP; *B*, [γ-^{32}P]ATP; *C*, [γ-^{35}S]ATP;*D*, representative Coomassie-stained gel showing the position and equal loading of the hMSH4 and hMSH5; *E*, UV cross-linking of hMSH4-hMSH5 (100 nM) with [γ-^{32}P]ATP (1 μM) in the presence or absence of Holliday Junction DNA (200 nM). Relative phosphorimager quantitation is shown: ○, hMSH4; ●, hMSH5.

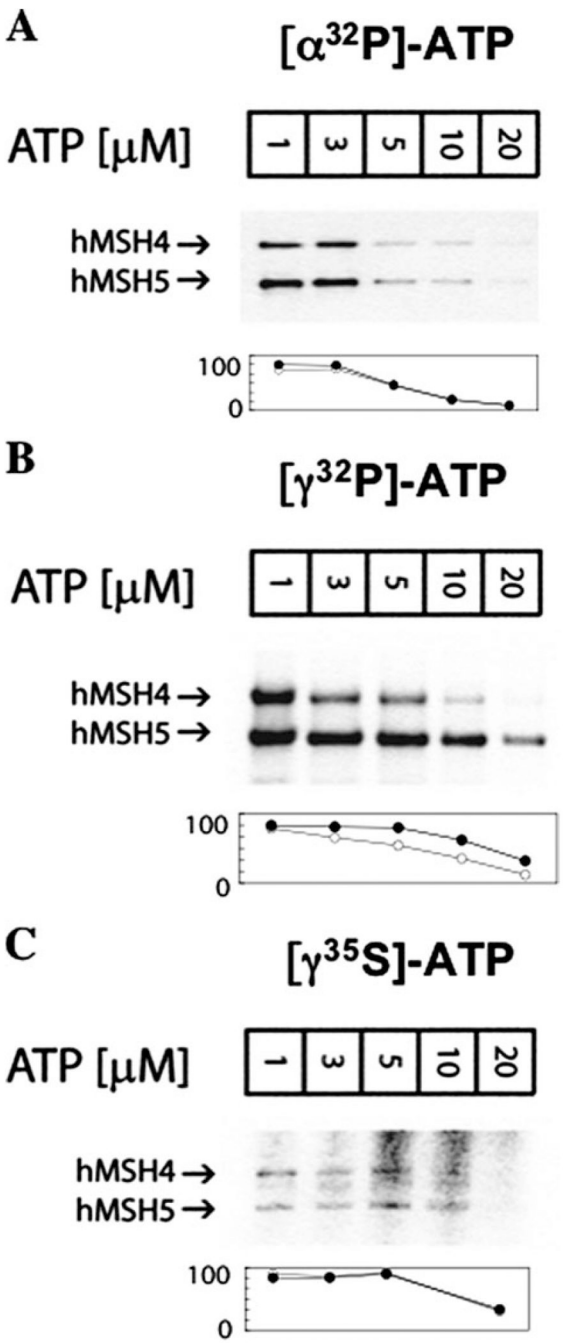

FIGURE 3. Competition of adenosine nucleotide cross-linking

hMSH4-hMSH5 (100 nM) was incubated with the labeled ATP (500 nM; see below), the indicated concentrations of unlabeled ATP (μM; shown in the *boxes above lanes*), and subjected to UV cross-linking. Reactions were separated on a 10% PAGE gel, visualized, and quantitated by phosphorimager (shown *below each panel*). *A*, [α-^{32}P]ATP ($S_{0.5(hMSH4)} \approx 4$ μM; $S_{0.5(hMSH5)} \approx 4$ μM); *B*, [γ-^{32}P]ATP ($S_{0.5(hMSH4)} \approx 3$ μM; $S_{0.5(hMSH5)} \approx 12$ μM); *C*, [γ-^{35}S]ATP ($S_{0.5(hMSH4)} \approx 7$ μM; $S_{0.5(hMSH5)} \approx 7$ μM). Relative phosphorimager quantitation is shown: ○, hMSH4; ●, hMSH5.

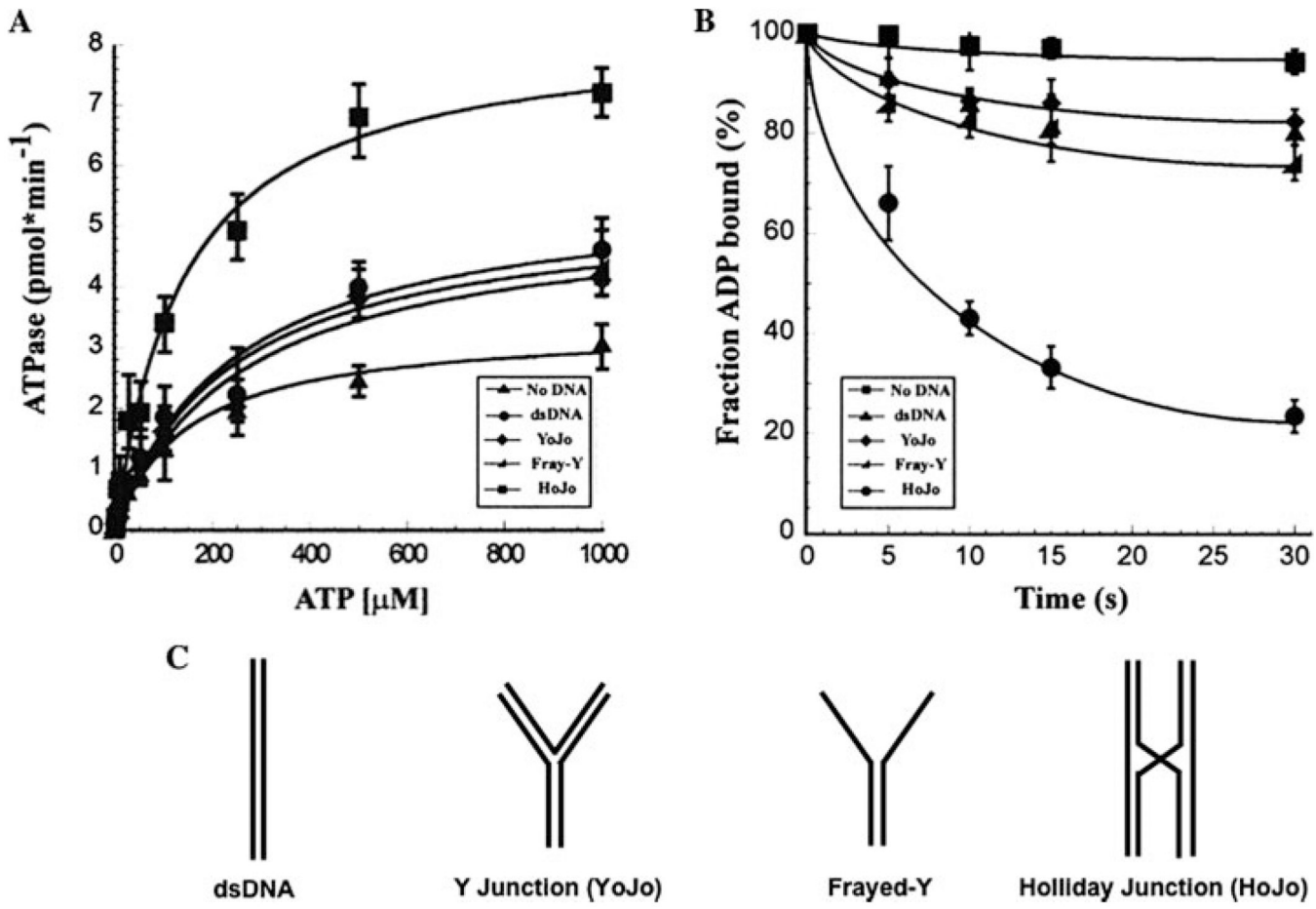

FIGURE 4. Holliday Junctions uniquely activate the hMSH4-hMSH5 steady-state ATPase and ADP → ATP exchange activities

A,DNA structure stimulation of the hMSH4-hMSH5 ATPase. Michaelis-Menten analysis of the hMSH4-hMSH5 (200 nM) ATPase activity was performed as previously described (11, 32) in the absence of DNA (▲), in the presence of duplex DNA (dsDNA, 600 nM; ●), Y-Junction DNA (YoJo, 600 nM; ♦), frayed Y-Junction DNA (Frayed-YoJo, 600 nM;), or Holliday Junction DNA (Hojo, 600 nM; ■) in a 20-μl reaction. *Error bars* indicate the standard deviation of at least three independent experiments. *B*,DNA structure provoked hMSH4-hMSH5 ADP → ATP exchange. hMSH4-hMSH5 was pre-bound to [^{3}H]ADP followed by the addition of 500 μM unlabeled ATP in the absence of DNA (■), in the presence of 3-fold excess duplex DNA (dsDNA, ▲), Y-Junction DNA(YoJo, ♦), frayed Y-JunctionDNA(Frayed-YoJo,), and Holliday JunctionDNA(HoJo, ●). Results are plotted as the fraction of total [^{3}H]ADP that remained bound over time. The standard of deviation was calculated from the average of at least four different concentrations of hMSH4-hMSH5 (25, 50, 75, and 100 nM) and from at least three independent experiments. *C*, diagram of substrates used in *A* and *B*.

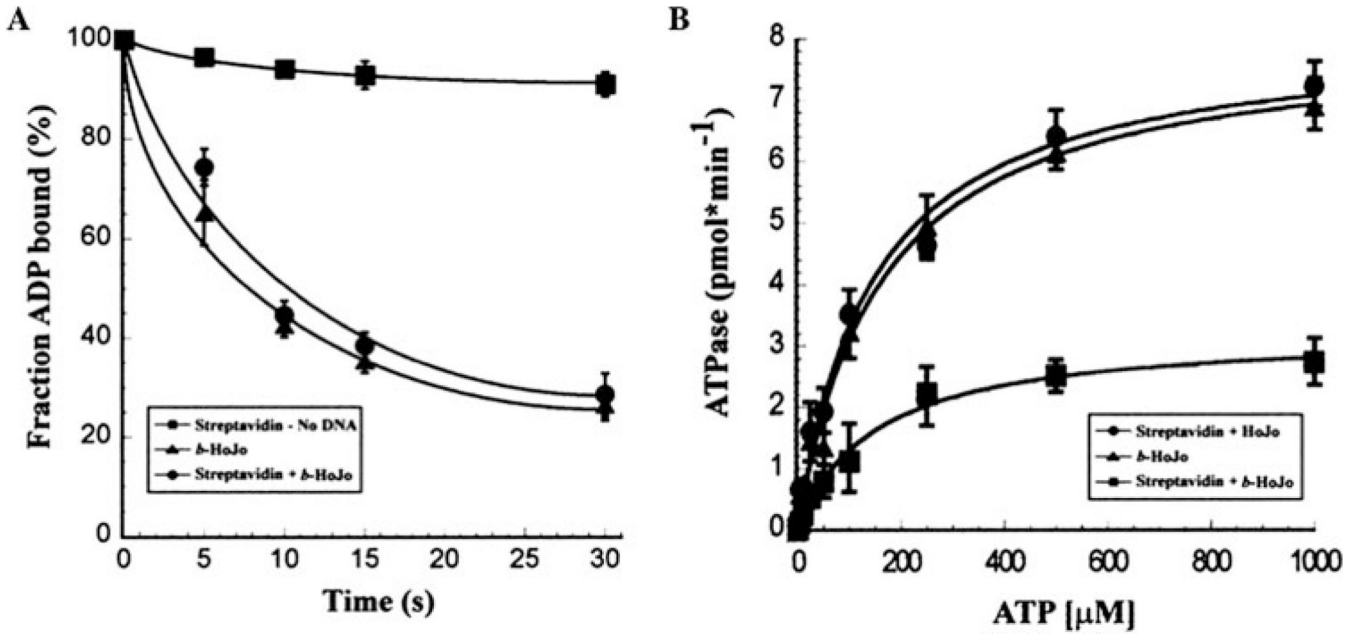

FIGURE 5. Blocking the Holliday Junction ends does not affect ADP → ATP exchange but does inhibit the steady-state ATPase of hMSH4-hMSH5

A, ADP → ATP exchange. Pre-steady state ADP → ATP exchange was performed as described under "Experimental Procedures" with hMSH4-hMSH5 (200 nM) in the absence of DNA but including streptavidin (800 μg/ml, ■), in the presence of HoJo DNA containing a 3′-biotin on the four DNA ends (*b*-Hojo, 600 nM, ▲), or in the presence of *b*-Hojo DNA (600 nM) including streptavidin (800 μg/ml, streptavidin +*b*-HoJo; ●). *Error bars* indicate the standard deviation of at least three independent experiments, which in some cases is within the symbol size. *B*, hMSH4-hMSH5 ATPase activity. Michaelis-Menten analysis of the hMSH4-hMSH5 (200 nM) ATPase activity was performed as previously described (11,32) in the presence of unbiotinylated HoJo DNA (600 nM) and including streptavidin (800 μg/ml; streptavidin + HoJo, ●), in the presence of HoJo DNA containing a 3′-biotin on the four DNA ends (600 nM; *b*-Hojo, ▲) or in the presence of *b*-Hojo DNA (600 nM) and including streptavidin (800 μg/ml; streptavidin+*b*-HoJo, ■). *Error bars* indicate the standard deviation of at least three independent experiments.

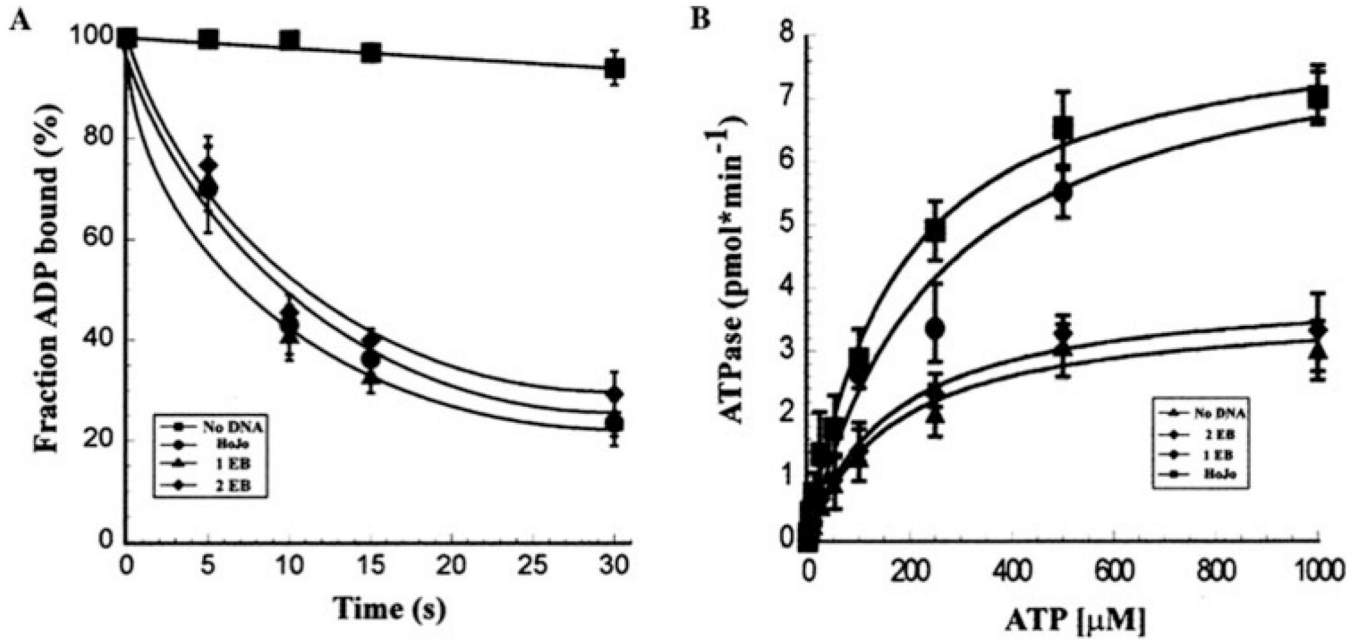

FIGURE 6. Blocking one duplex arm on both ends of a Holliday Junction stacked-duplex does not affect hMSH4-hMSH5 ADP → ATP exchange but inhibits ATPase activity

A, ADP → ATP exchange by hMSH4-hMSH5 is unaffected by the disposition of HoJo ends. Pre-steady state ADP → ATP exchange was performed as described under "Experimental Procedures" with hMSH4-hMSH5 (200 n_M) in the absence of DNA (■) or in the presence of HoJo DNA (600 n_M,●), single end-blocked stacked-duplex HoJo DNA (1EB, 600 n_M, ♦), or double end-blocked stacked-duplex HoJo DNA (2EB, 600 n_M, ▲). *B*, hMSH4-hMSH5 ATPase activity requires an open-end HoJo stacked duplex. Michaelis-Menten analysis of the hMSH4-hMSH5 (200 n_M) ATPase activity was performed as previously described (11,32) in the absence of DNA (▲) or in the presence of HoJo DNA (600 n_M, ■), single end-blocked stacked-duplex HoJo DNA (1EB, 600 n_M, ●), or double end-blocked stacked-duplex HoJo DNA (2EB, 600 n_M,♦). *Error bars* indicate the standard deviation of at least three independent experiments.

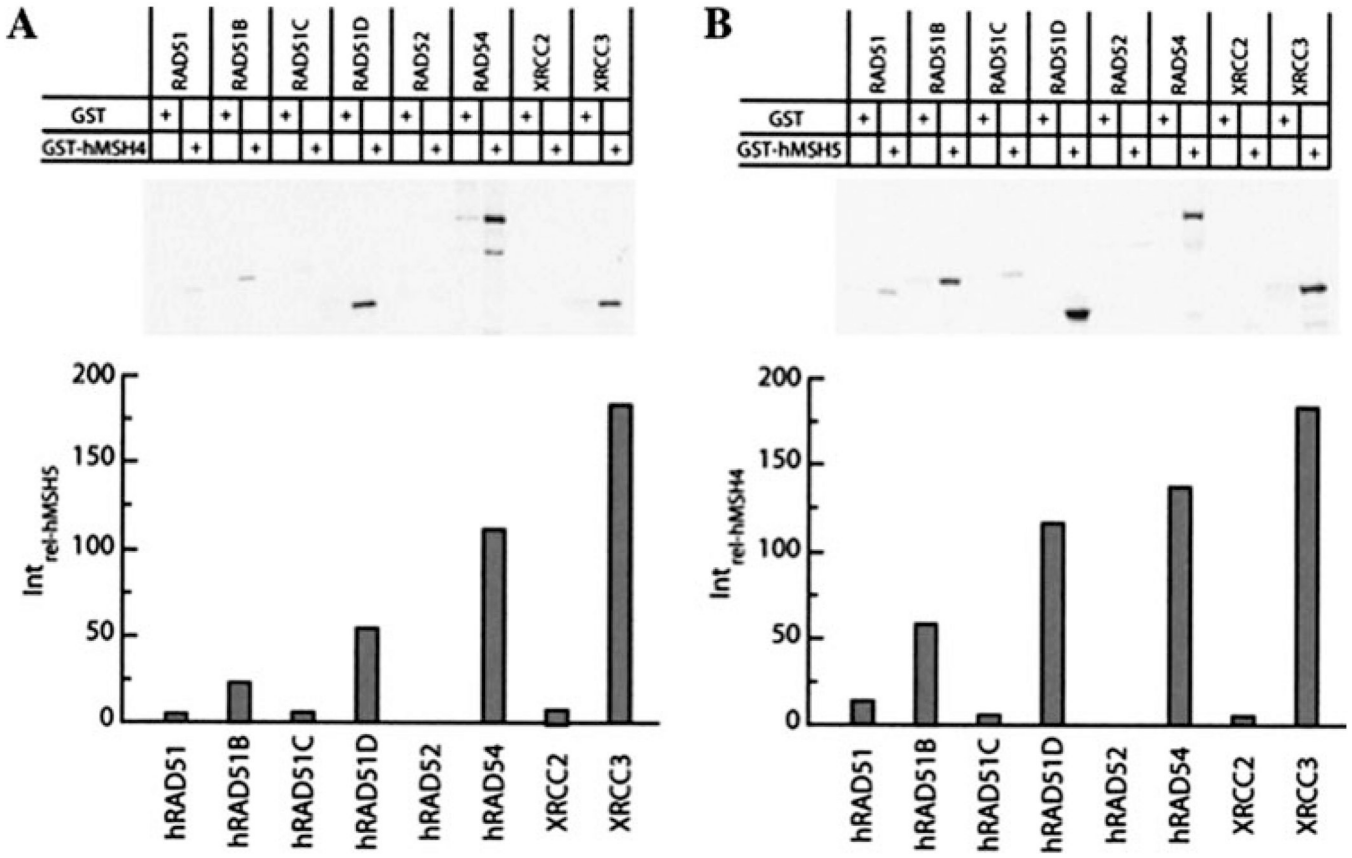

FIGURE 7. Interactions between hMSH4 and hMSH5 with homologous recombination machinery

A, interaction of DSB repair proteins with hMSH5. [^{35}S]Methionine-labeled IVTT proteins were quantitated relative to the number of methionine residues in each protein and equimolar amounts were precipitated with an excess of purified GST-hMSH4 protein. GST alone was used as a precipitation control. *Upper panel* shows the gel of precipitated IVTT proteins. Precipitated material was quantitated by phosphorimager, nonspecific GST-only interaction subtracted, and the remaining interaction calculated relative to the known interactor hMSH5 ($Int_{rel(hMSH5)}$) and plotted in the lower panel. *B*, interaction of DSB repair proteins with hMSH4. [^{35}S]Methionine-labeled IVTT proteins were quantitated relative to the number of methionine residues in each protein and equimolar amounts precipitated with an excess of purified GST-hMSH5 protein. GST alone was used as a precipitation control. *Upper panel* shows the gel of precipitated IVTT proteins. Precipitated material was quantitated by phosphorimager, nonspecific GST-only interaction subtracted, the remaining interaction calculated relative to the known interactor hMSH4 ($Int_{rel(hMSH4)}$) and plotted in the *lower panel*